Tetrahedron Vol. 49, No. 24, pp. 5377-5396, 1993
Printed in Great Britain

0040-4020/93 $6.00+.00

Racemate Resolution via Crystallization of Diastereomeric Salts: Thermodynamic Considerations and Molecular Mechanics Calculations

Frank J. J. Leusen*, Jan H. Noordik and Heinrich R. Karfunkel†

CAOS/CAMM Center, University of Nijmegen, Toernooiveld, NL-6525 ED Nijmegen, The Netherlands

* Author to whom correspondence should be addressed. Present address: Molecular Simulations Inc.,
St. John's Innovation Centre, Cowley Road, Cambridge CB4 4WS, United Kingdom

† Information Technology Department, Ciba-Geigy AG, R-1008.823, CH-4002 Basel, Switzerland

(*Received in UK* 15 *March* 1993)

Abstract: It is of crucial importance in many areas of (bio)chemistry to use enantiomerically pure substances. On an industrial scale, enantiopure compounds are often produced by resolution of racemic mixtures via crystallization of diastereomeric salts. The technique is still applied on a trial and error basis. In this paper, we present a thermodynamic approach which shows that resolution efficiency is related to the lattice energy difference in a pair of diastereomeric salts. Application of this line of reasoning to an extensive series of closely related resolutions allows for a qualitative rationalization of these resolutions. Reliable quantitative calculations by means of computer assisted crystal modeling are not (yet) possible due to inaccuracies of present computational techniques, but such calculations may be successful in the near future, and a truly predictive model for racemate resolutions becomes feasible.

1 — INTRODUCTION

The chiral chemistry of live[1] often necessitates the use of enantiomerically pure compounds (e.g., in pharmacy, agriculture, cosmetics and nutrition).[2–5] If a target compound can not be isolated from natural products and stereoselective synthesis is too complicated (or too expensive), a racemic mixture of either the end-product or a precursor may be resolved into enantiopure substances. There are several ways to resolve racemates, which have been comprehensively discussed in recent literature.[6,7] For resolutions on an industrial scale, crystallization techniques are preferred, in particular selective crystallization of diastereomers.[6] This separation technique is based on the solubility difference in a pair of diastereomeric salts. The method is sometimes denoted "classical" resolution as it was first performed by Pasteur in 1853, when he resolved racemic mixtures of tartaric acid with the alkaloid-derivatives quinicine and cinchonidine.[8,9] Nowadays, several useful resolving agents are known, among which a considerable number of natural products, such as alkaloids and naturally occurring acids.[10,11] The term "classical" resolution may erroneously imply that the ins and outs of the technique are completely understood. In contrast, finding a suitable resolving agent for a given racemate is still mainly a matter of trial and error.[10] A reliable predictive tool is needed in order to understand, and ultimately design, resolutions. Several studies aiming at rationalizing resolutions are reported in recent literature (e.g.,[12-16]), but the predictive abilities are still limited.

In this contribution, we present a thermodynamic approach to rationalize "classical" resolutions. This approach links resolution efficiency and lattice energy difference in a diastereomeric salt-pair. The model is applied to an unique series of 14 resolutions analyzed previously,[17-21] and will be discussed after a brief introduction to the experimental data of these resolutions. Use of the model, in a careful analysis of diastereomeric pairs of X-ray structures, allows for the qualitative rationalization of our series of resolutions. In an attempt to arrive at more quantitative results, we investigated the reliability of present Molecular Mechanics (MM) methodologies in computing the lattice energy difference in a diastereomeric pair as a parameter for resolution efficiency. Finally, a possible path towards a truly predictive model for "classical" resolutions is outlined.

2 — EXPERIMENTAL DATA

The synthetic cyclic phosphoric acids (see Figure 1) are excellent resolving agents towards amines and amino acids.[17] We selected them for a systematic investigation of the resolution of the alkaloid ephedrine.[22] The study includes 14 resolutions of 11 unsubstituted and 3 substituted ephedrines with the unsubstituted–, six halogen-substituted– and four otherwise substituted cyclic phosphoric acids. Physical data of the 28 diastereomeric salts have been published previously.[18,21] For convenience, the differences in relevant physical properties are summarized in Table 1, together with the efficiency of each resolution, which is described by the parameter $\ln(c_p/c_n)$, where c_p and c_n are the solubilities of p-salt and n-salt. This parameter follows from thermodynamic considerations discussed in Section 3.1.

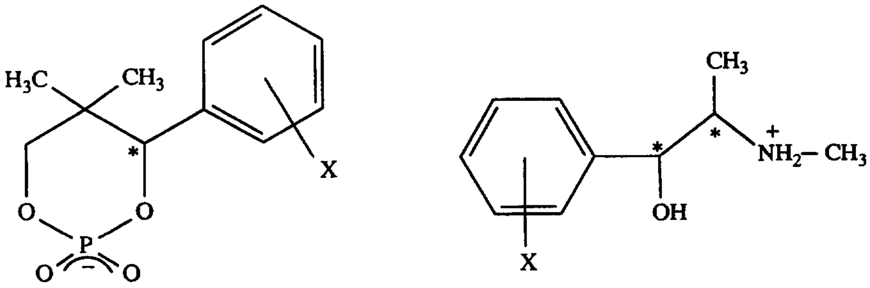

Figure 1: Structures of the cyclic phosphoric acids (left) and ephedrine (right). Aromatic substituents are given in Table 1.

Table 1: Experimental Data.

Acid phenyl subst.	Base phenyl subst.	$\ln(c_p/c_n)$ [a] EtOH	i-PrOH	PrOH	ΔD [b] $\left(\frac{g}{cm^3}\right)$	ΔM.p. [c] (K)	$\Delta\Delta H_f$ [d] $\left(\frac{kcal}{mol}\right)$
H	H	−0.05	−0.05	−0.02	−0.007	−4.2	0.2±0.4
2-F	H	0.73	0.81	–	−0.003	8.8	0.8±0.1
2-Cl	H	1.42	1.37	1.43	0.020	1.4	2.0±0.4
2-Br	H	0.57	0.55	–	0.015	9.6	0.5±0.3
2,6-diCl	H	1.83	1.69	–	0.013	12.1	2.1±0.9
2,4-diCl	H	1.81	1.78	1.84	0.057	31.4	4.4±0.3
2-OCH_3	H	1.73	1.61	1.76	–	20.1	0.9±0.4
2-NO_2	H	−0.43	−0.59	−0.40	–	−7.1	−1.1±0.1
2-CH_3	H	1.11	1.06	1.13	–	−11.3	1.9±0.3
4-Cl	H	2.08	2.18	–	–	32.4	2.6±0.4
4-CH_3	H	0.13	0.19	–	–	0.1	0.7±0.4
H	2-Cl	–	−0.10	–	–	7.2	−1.4±0.1
2-Cl	2-Cl	–	2.49	–	–	56.2	3.5±0.3
2-Cl	4-Cl	–	−1.02	–	–	−40.5	−0.5±0.6

---

[a] See Section 3.1 for explanation of $\ln(c_p/c_n)$ which describes resolution efficiency. Solubility concentrations (c_n for n-salt and c_p for p-salt) were measured at 298.15 K, the error is smaller than 3%.[18,21]

[b] Difference in density, measured in mixtures of xylene and CCl_4 at 294.7 K using the floatation method.[18]

[c] Melting points (M.p.) and heats of fusion (ΔH_f) were measured on a Perkin Elmer DSC 7 Differential Scanning Calorimeter.[18,21]

[d] Differences in properties are calculated by subtracting the value of the p-salt from that of the n-salt, i.e., for the difference in heat of fusion $\Delta\Delta H_f = \Delta H_{f(n)} - \Delta H_{f(p)}$. Throughout the text, $\Delta\Delta H_f$ will refer to the experimental value.

In most cases, the p-salt[24] is more soluble, has the lower melting point and the smaller enthalpy of fusion. In general, the chlorine substituted acids appear to be the better resolving agents. The efficiency of the resolution of ephedrine by the phosphoric acids appears to be independent of the solvents used here (the compounds do not dissolve in less protic or less polar solvents). This solvent independence allows us to focus on solubilities in i-PrOH only, since that set is complete. Furthermore, it suggests that the chiral discrimination is not a solution-determined property, but manifests itself mainly in the solid state. Crude estimates of the differences in structural properties of the diastereomeric salt-pairs are provided by differences in density (ΔD, measure of crystal packing efficiency), differences in melting point (ΔM.p., measure of intermolecular interactions) and differences in heat of fusion ($\Delta\Delta H_f$, which combines ΔD and ΔM.p. into a measure for lattice energy differences). The results in Table 1 show no relationship between resolution efficiency $\ln(c_p/c_n)$ and ΔD or ΔM.p., but a significant correlation between $\ln(c_p/c_n)$ and $\Delta\Delta H_f$ with a correlation coefficient of 0.869 (n = 14), as visualized in Figure 2.

This empirical relationship between two experimentally accessible parameters describing the resolution process will be used furtheron to correlate resolution efficiency and a computationally accessible energy parameter. The subtle interplay of interactions which determines the result of a resolution should be described by all contributions and not only those provided by $\Delta\Delta H_f$. Entropy effects, for instance,

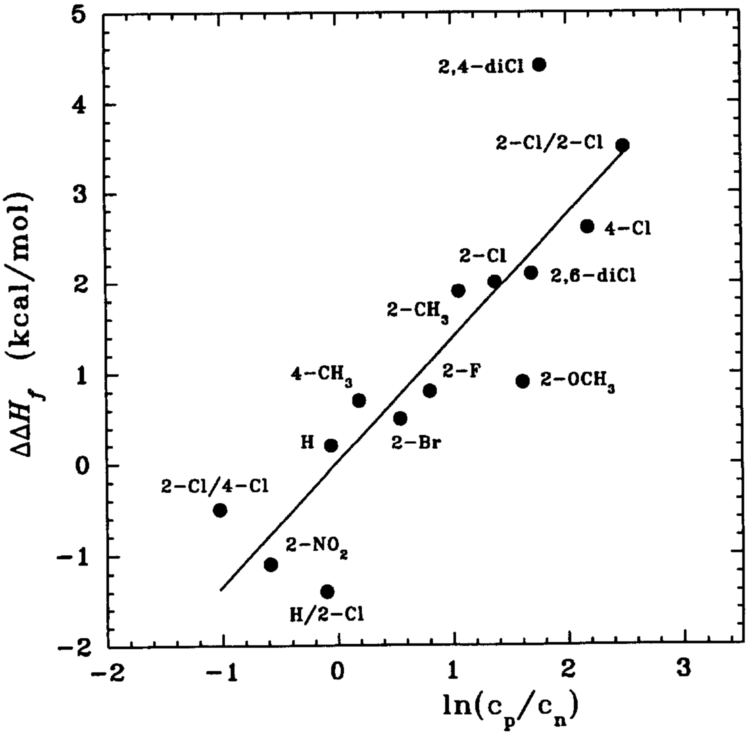

Figure 2: Plot of $\Delta\Delta H_f$ versus ln(c$_p$/c$_n$). Labels indicate acid substituents (with unsubstituted ephedrine) or acid/base phenyl substituents.

may also be important if the crystal packing is different for the two salts of a pair. Therefore, thermodynamic aspects of resolutions will be considered in the next section.

3 — THERMODYNAMIC CONSIDERATIONS

3.1 Resolution efficiency

The efficiency of a resolution process is obviously determined by the following solvation equilibria of n- and p-salt:

$$[A^+B^-]_{\mathrm{solid(n)}} \overset{k_{1(n)}}{\rightleftharpoons} [A^+B^-]_{\mathrm{solution(n)}} \overset{k_{2(n)}}{\rightleftharpoons} [A^+]_{\mathrm{solution(n)}} + [B^-]_{\mathrm{solution(n)}}$$
$$[A^+B^-]_{\mathrm{solid(p)}} \overset{k_{1(p)}}{\rightleftharpoons} [A^+B^-]_{\mathrm{solution(p)}} \overset{k_{2(p)}}{\rightleftharpoons} [A^+]_{\mathrm{solution(p)}} + [B^-]_{\mathrm{solution(p)}} \qquad (1)$$

where A^+ and B^- are the acid and the base ion, respectively. The subscript "solid" represents the diastereomeric salt and "solution" represents the saturated solution. If the difference in pK$_a$ values between acid and base is large enough (as is the case for the ephedrine (pK$_a$ = 10)[26] – cyclic phosphoric acid (pK$_a$ = 2–3)[27,28] systems), the Gibbs free energies of solvation are related directly to the equilibrium constants $K_{solv(n)} = k_{1(n)} \cdot k_{2(n)}$ and $K_{solv(p)} = k_{1(p)} \cdot k_{2(p)}$. As a result, $K_{solv} = \frac{[\mathrm{A}^+]_{\mathrm{solution}} \cdot [\mathrm{B}^-]_{\mathrm{solution}}}{[\mathrm{A}^+\mathrm{B}^-]_{\mathrm{solid}}} \equiv [\mathrm{A}^+]_{\mathrm{solution}} \cdot [\mathrm{B}^-]_{\mathrm{solution}}$ for both salts, since $[\mathrm{A}^+\mathrm{B}^-]_{\mathrm{solid}} \equiv 1$.[29] Thus, $K_{solv(n)} = \mathrm{c_n} \cdot \mathrm{c_n}$ and $K_{solv(p)} = \mathrm{c_p} \cdot \mathrm{c_p}$, and the difference in Gibbs free energy of solvation for a pair of diastereomeric salts, $\Delta\Delta G_{solv}$, can be calculated using $\Delta G_{solv} = -RT\ln(K_{solv})$:

$$\begin{aligned} \Delta\Delta G_{solv} &= \Delta G_{solv(n)} - \Delta G_{solv(p)} \\ &= RT\ln(\mathrm{c_p^2}) - RT\ln(\mathrm{c_n^2}) \\ &= 2RT\ln(\mathrm{c_p}/\mathrm{c_n}) \end{aligned} \tag{2}$$

This relationship links the energetical aspect of the resolution process with the solubilities of the two diastereomeric salts. Because none of the parameters commonly used to describe resolution efficiency (e.g., $\mathrm{S} = (\mathrm{c_p} - \mathrm{c_n})/\mathrm{c_p}$)[12,18,30] shows such a (linear) relationship with the energetical aspect of the resolution process, we propose the parameter $\ln(\mathrm{c_p}/\mathrm{c_n})$ as such. Relationship 2 forms the basis for the rationalization of optical resolutions using MM techniques.

3.2 Resolution efficiency versus lattice energy difference

$\Delta\Delta G_{solv}$ (and thus $\ln(\mathrm{c_p}/\mathrm{c_n})$) can not be calculated with present computational techniques.[31] However, it follows from equation 2 and the empirical relationship of Figure 2 that the lattice energy difference in a diastereomeric pair is related to $\Delta\Delta G_{solv}$. This lattice energy difference is, in principle, computationally accessible. Consider two salts forming a diastereomeric pair, denoted n-salt and p-salt, in solid state, in liquid state (the melt) and in solution:

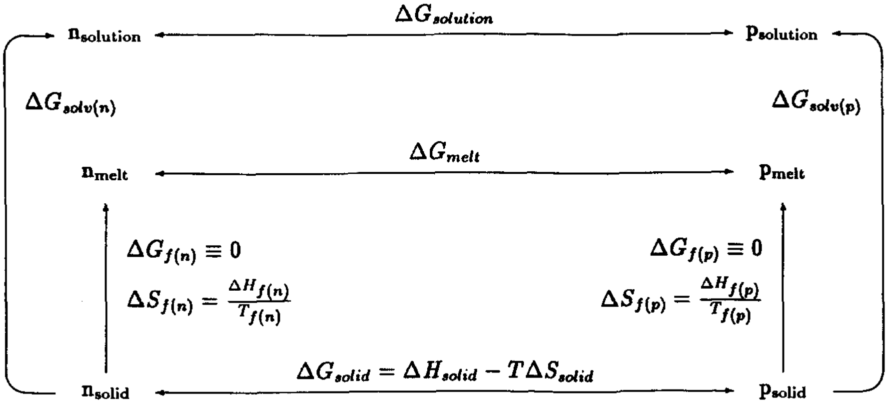

where ΔG_{solid} denotes the free energy difference between the two salts in solid state, and comparable definitions are used for ΔG_{melt} and $\Delta G_{solution}$. The free energies of solvation are represented by $\Delta G_{solv(n)}$ and $\Delta G_{solv(p)}$ for n-salt and p-salt, respectively. Similarly, $\Delta H_{f(n)}$ and $\Delta H_{f(p)}$ are the heats of fusion, and $T_{f(n)}$ and $T_{f(p)}$ are the melting points.

The outer thermodynamic cycle, from $\mathrm{n_{solid}}$ via $\mathrm{n_{solution}}$ and $\mathrm{p_{solution}}$ to $\mathrm{p_{solid}}$, describes the resolution process. Available experimental data indicate that the dissolved ephedrine–phosphoric acid salts are completely dissociated and solvated. The following data supports this assumption:

(i) The resolution efficiency is found to be independent of the solvent used (see Table 1);
(ii) The difference in pK_a-values is sufficiently large ($\Delta pK_a \geq 7$); and
(iii) ^{13}C and ^{31}P NMR measurements on some of the salts, solved in methanol in concentrations as high as possible, showed no differences at all in resonances (results not shown).
Thus there is no inter-ionic interaction in solution, and $\Delta G_{solution}$ is negligibly small. Subsequently,[32]

$$\Delta\Delta G_{solv} = (\Delta G_{solv(n)} - \Delta G_{solv(p)}) \approx -\Delta G_{solid} \tag{3}$$

ΔG_{solid}, and thereby also $\ln(c_p/c_n)$ as a parameter for resolution efficiency, is computationally accessible in principle, but computation of the Gibbs free lattice energy with MM (i.e., crystal dynamics) is very demanding. However, computational demands can be reduced by separate consideration of the approximated entropy contribution to ΔG_{solid} using the inner Born-Haber cycle, which describes the melting processes. The resulting lattice enthalpy difference ΔH_{solid} is accessible by MM lattice energy minimizations, provided the availability of reliable force fields and minimization techniques. Details of the necessary approximations will be discussed furtheron, but two important assumptions should be mentioned here:
(i) $\Delta G_{melt} \ll \Delta G_{solid}$ ($\Delta H_{melt} \ll \Delta H_{solid}$ and $T\Delta S_{melt} \ll T\Delta S_{solid}$) since, in comparison to the (ordered) solid states n_{solid} and p_{solid}, the melts will show less stereoselective interactions, which, in addition, cancel each other due to random ordering of the ions in n_{melt} and p_{melt}.
(ii) Although the temperature is not invariant in the inner thermodynamic cycle, the entropy dependence on temperature is not accounted for. This assumption is justified because the effect will be very similar for both salts and is mainly due to the difference in melting points between n– and p-salt, which is not large for the compounds studied.
Under these approximations, and with $\Delta G_f \equiv 0$ and therefor $\Delta S_f \equiv \frac{\Delta H_f}{T_f}$[29] at equilibrium, the entropy term $T\Delta S_{solid}$ is calculated from the fusion cycle according to:

$$T\Delta S_{solid} \approx -T\Delta\Delta S_f = -T \cdot (\Delta S_{f(n)} - \Delta S_{f(p)}) = -T \cdot \left(\frac{\Delta H_{f(n)}}{T_{f(n)}} - \frac{\Delta H_{f(p)}}{T_{f(p)}}\right) \tag{4}$$

ΔG_{solid} values, computed from the solubility data in Table 1 according to equations 2 and 3, $T\Delta S_{solid}$ values, calculated from the melting point and heat of fusion data in Table 1 according to relationship 4, and ΔH_{solid} data, obtained using

$$\Delta H_{solid} = \Delta G_{solid} + T\Delta S_{solid} \approx -(\Delta\Delta G_{solv} + T\Delta\Delta S_f) \tag{5}$$

are listed in Table 2 for the 14 ephedrine–phosphoric acid resolutions. The high degree of correlation between $\ln(c_p/c_n)$ and ΔH_{solid} (R = 0.954 with n = 14, see Figure 3) indicates that the computationally accessible ΔH_{solid} can be confidently used as a parameter for resolution efficiency.

In summary, the thermodynamic approach presented above links the experimental difference in heat of fusion $\Delta\Delta H_f$, the experimentally accessible lattice enthalpy difference ΔH_{solid}, the computationally accessible lattice energy difference and the racemate resolution efficiency $\ln(c_p/c_n)$ to each other. This makes measured lattice enthalpy differences (ΔH_{solid}) good test values for the reliability of MM methods to compute lattice energies of these organic salts.[33] If present MM methods prove sufficiently reliable, observed resolutions can be rationalized quantitatively according to the relationship of Figure 3.

Table 2: Application of the Thermodynamic Approach to Ephedrine–Cyclic Phosphoric Acid Resolutions.

Acid subst.	Base subst.	$\ln(c_p/c_n)$[a]	ΔG_{solid}[b] $\left(\frac{kcal}{mol}\right)$	$T\Delta S_{solid}$[c] $\left(\frac{kcal}{mol}\right)$	ΔH_{solid}[d] $\left(\frac{kcal}{mol}\right)$
H	H	-0.05	0.06	-0.17	-0.11
2-F	H	0.81	-0.96	-0.40	-1.35
2-Cl	H	1.37	-1.63	-1.20	-2.82
2-Br	H	0.55	-0.65	-0.19	-0.84
2,6-diCl	H	1.69	-2.00	-1.16	-3.17
2,4-diCl	H	1.78	-2.10	-2.36	-4.46
2-OCH_3	H	1.61	-1.90	-0.27	-2.18
2-NO_2	H	-0.59	0.69	0.57	1.26
2-CH_3	H	1.06	-1.26	-1.32	-2.57
4-Cl	H	2.18	-2.59	-1.13	-3.72
4-CH_3	H	0.19	-0.23	-0.43	-0.66
H	2-Cl	-0.10	0.12	0.94	1.05
2-Cl	2-Cl	2.49	-2.96	-1.24	-4.20
2-Cl	4-Cl	-1.02	1.21	-0.26	0.94

---

[a] Resolution efficiency in i-PrOH at 298.15 K.

[b] As explained in the text, $\Delta G_{solid} \approx -\Delta\Delta G_{solv} = -2RT\ln(c_p/c_n)$, with $R = 1.987$ cal/mol · K and $T = 298.15$ K.

[c] Calculated from experimental data in Table 1: $T\Delta S_{solid} \approx -T(\Delta H_{f(n)}/T_{f(n)} - \Delta H_{f(p)}/T_{f(p)})$, with $T = 298.15$ K.

[d] $\Delta H_{solid} = \Delta G_{solid} + T\Delta S_{solid}$.

3.3 Summary of approximations used

The presented thermodynamic approach assumes complete dissociation of the salts in solution, which is the case for combinations of strong acids and bases, e.g., the ephedrine–phosphoric acid resolutions. Incomplete dissociation (weak acid or base) would probably result in a lower accuracy, since the ions do interact in solution and as a result $\Delta G_{solution} \neq 0$. The entropy effect due to the solubility difference in a diastereomeric salt-pair may also cause $\Delta G_{solution}$ to be non-zero: in case of a large difference in solubility, the saturated solutions have different numbers of solute molecules per unit of volume, i.e., $\Delta S_{solution} \neq 0$ and thus $\Delta G_{solution} \neq 0$. Note that this deviation affects only the slope — and not the accuracy — of the relationship of Figure 3, since $\Delta S_{solution}$ is a function of the solubility ratio. Furthermore, this entropy effect is expected to be quite small in the present study, because the solubilities in i-PrOH are low (less than 0.15 mol/l).

Two other important approximations, i.e., $\Delta G_{melt} \ll \Delta G_{solid}$ and the neglect of the entropy dependence on temperature in the range between the two melting points, were addressed earlier. The latter approximation, however, is not essential to the model since a proper correction term could be included if the experimental heat capacities of the diastereomeric salts were available.

Specific thermodynamic effects resulting from inclusion of solvent molecules in the lattice are not accounted for, because this leads to an impractical complexity. If only one salt of a pair contains solvent

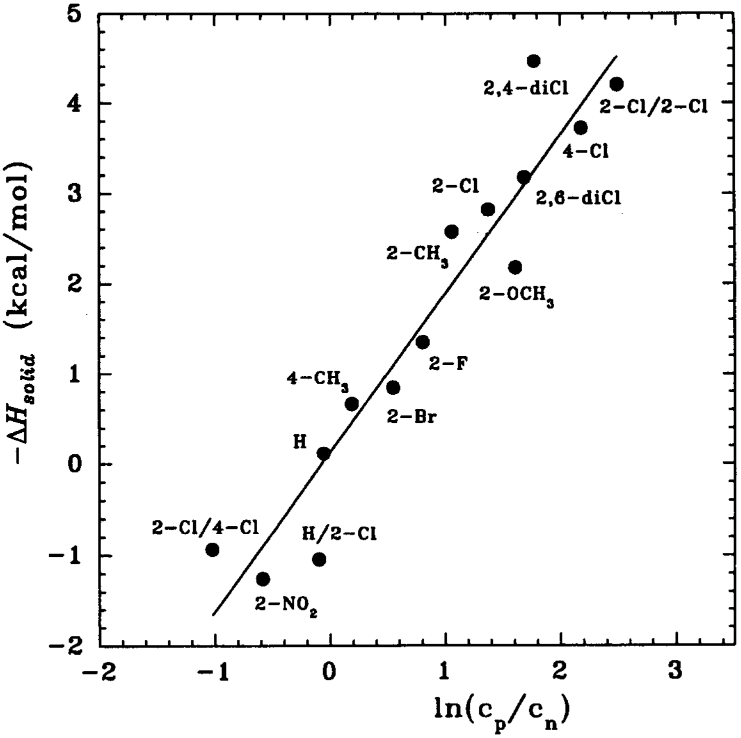

Figure 3: Plot of $-\Delta H_{solid}$ versus $\ln(c_p/c_n)$. Labels indicate acid substituents (with unsubstituted ephedrine) or acid/base phenyl substituents. The deviations of the individual points from the line indicate the variation in $T\Delta S_{solid}$, and are also caused by the error in the entropy approximation used.

molecules, the accuracy of the relation might be negatively influenced. On the other hand, our test set of structures (which includes several solvent containing salts) shows a high correlation between resolution efficiency and lattice enthalpy difference, which is an indication of the validity of neglecting included solvent effects in the resolutions studied here. Nevertheless, the thermodynamic considerations of solvent molecules included in the lattice merit further and more detailed investigation.

Some protocols to use the presented relationship between ΔH_{solid} and $\ln(c_p/c_n)$ to rationalize (and ultimately predict) racemate resolutions are outlined in the next sections. The ephedrine–phosphoric acid resolutions are used as a test case.

4 — THE QUALITATIVE APPROACH

The thermodynamic model can be used to evaluate resolution efficiency by comparison of X-ray structures of diastereomeric salt-pairs. Estimates of lattice enthalpy differences can be determined qualitatively by analyzing differences in interactions between the structures. This qualitative approach is commonly used to understand resolutions.[34-38] The first six ephedrine–phosphoric acid resolutions listed in Table 1 were studied in this way. The twelve crystal structures[39–45] can be divided into three distinct classes of crystal packing; details of these packing modes have been published previously.[20] All structures show alternating hydrophilic and hydrophobic layers, but the distances between the layers are different.[46]

Class I contains seven very similarly packed diastereomeric salts; minor differences between the n-salts (Class I_n) and p-salts (Class I_p) originate from the different orientation of the phenyl rings of the ephedrine enantiomers in the hydrophobic layers. The inter-layer distance of the Class I compounds is about 14 Å. Class II contains three p-salts which are structurally dissimilar (inter-layer distances of 12.6, 15.4 and 16.4 Å), but they all have water molecules included in the lattice and exhibit an inefficient crystal packing. The two remaining n-salts are isostructural. These Class III salts are packed very efficiently (inter-layer distance of 10 Å) and show more close Van der Waals (VdW) contacts than the other compounds.

The solubility order of the three classes of crystal packing (Class II > Class I > Class III) reflects the lattice energy ordering. These energetical differences are not due to differences in strong intermolecular interactions (e.g., hydrogen bonds) or conformational differences of the ions.[20] However, inclusion of crystal water in one diastereomeric salt of a pair (Class II) and/or subtle differences in weak intermolecular interactions (such as VdW contacts in Class III)[19] appear to be important for resolution efficiency (See Table 3). The resolution is poor if there is no difference in packing mode, as for the unsubstituted acid where both salts are in the Class I packing. A good resolution of ephedrine is accomplished when the difference in packing efficiency is considerable, like in the salts with the 2-Cl substituted acid (n-salt: efficient Class III packing, p-salt: standard Class I_p packing) and the 2,6-diCl substituted compound (n-salt: standard Class I_n, p-salt: inefficient Class II). The excellent resolution by the 2,4-diCl substituted acid is explained by the large difference in packing efficiency between the n-salt (efficient Class III) and the p-salt (inefficient Class II).

The packing differences in these pairs of diastereomers agree with the entropy differences calculated according to equation 4. $T\Delta S_{solid}$ (Table 2) is small if the difference in packing efficiency is small, as is the case for the diastereomeric pairs with the unsubstituted and the 2-F substituted acid. If there is a significant entropy contribution to ΔG_{solid}, a difference in packing efficiency is found, e.g., –1.2 kcal/mol for the 2-Cl substituted acid, which must be mainly attributed to the tight packing of acid and base

Table 3: Relationship between Crystal Packing Modes of the Diastereomeric Salts and Resolution Results. Note the solubility order of the salts: Class II > Class I > Class III.

Acid phenyl Substituent	$\ln(c_p/c_n)$	Packing mode n-salt	Packing mode p-salt	Resolution Cause
H	–0.05	I_n	I_p	None
2-F	0.81	I_n	I_p	Polarization effects
2-Cl	1.37	III	I_p	Van der Waals forces
2-Br	0.55	I_n	II	Solvent inclusion
2,6-diCl	1.69	I_n	II	Solvent inclusion
2,4-diCl	1.78	III	II	Van der Waals forces and solvent inclusion

phenyl moieties in the hydrophobic layers of the n-salt (Class III) versus the relatively loose packing of these groups in the hydrophobic layers of the p-salt (Class I_p). Inclusion of solvent in the lattice of the p-salt results in an entropy contribution of about -1.2 kcal/mol in case of the 2,6-diCl substituted compound (Class I_n versus Class II). Surprisingly, $T\Delta S_{solid}$ is quite small for the 2-Br substituted acid (-0.2 kcal/mol), although the p-salt contains even two crystal water molecules. A markedly higher value was expected. Whether this discrepancy is caused by crystallographic disorder of the included solvent, or some other reason, is yet unclear. It emphasizes, however, that the energetic role of solvent molecules included in the lattice is complicated and merits further research. The largest entropy term (-2.4 kcal/mol) is found in the resolution of ephedrine by the 2,4-diCl substituted acid (Class III versus Class II). Apparently, this entropy difference is composed of the packing difference in the hydrophobic layers (-1.2 kcal/mol) and inclusion of crystal water in the p-salt (also -1.2 kcal/mol).

Of course, one cannot expect very precise results from the qualitative approach, because all intermolecular interactions other than short-range VdW, hydrogen bonding and electrostatic contacts are not considered in this evaluation. The qualitative approach is, for instance, too general to explain the large difference in resolution results with the 2-Br substituted acid in comparison to the 2,6-diCl substituted acid (both Class I_n versus Class II). In order to obtain a more detailed and quantitative insight into the intermolecular forces (including long-range interactions) governing these optical resolutions, lattice energy calculations are presented in the next section.

5 — THE QUANTITATIVE APPROACH

The lattice energy difference ΔH_{solid} in a diastereomeric salt-pair (and thus the resolution efficiency) can be calculated using MM techniques, provided the availability of X-ray data. Methodology to predict crystal packing (see furtheron) is a prerequisite for a fully predictive model describing racemate resolution. However, lattice energy computations are not trivial and we have shown previously that standard MM methods are not sufficiently reliable to reproduce the expected lattice enthalpy differences.[20] Even the X-ray structures of some of the diastereomeric salts studied could not be reproduced using standard MM. In the next sections, we present the results of a series of calculations on two pairs of diastereomeric salts (containing the unsubstituted and the 2-Cl substituted cyclic phosphoric acid) using a non-standard force field.

5.1 Computational methods

CHARMm version 21.3[47,48] was employed, with the following modifications:[49]
(i) *Ab initio* Electrostatic Potential (ESP)[50-52] derived atomic charges were used. ESPs were obtained using *ab initio* Gaussian-90[53] (6-31G** basis set) calculations on the separate ions, and atomic charges were derived from these ESPs by the QCPE program PDM88.[54,55] Since the ions are very large to be treated with *ab initio* methods, full geometry optimization with Gaussian appeared to be computationally too demanding. This problem was tackled by first optimizing hydrogen positions of the separate ions using CHARMm (all non-hydrogens were kept fixed to their X-ray coordinates and Quanta template charges[56] were applied). The resulting structures were then subjected to one SCF calculation with

Gaussian-90 (6-31G** basis set) to obtain the ESPs, and atomic charges were derived using PDM88. Subsequently, the diastereomeric salts were CHARMm minimized with these charges and the resulting conformers of the ions were subjected to an additional series of Gaussian-ESP calculations to obtain the final charge-set.

(ii) To handle a larger number of atom-atom interactions than usual, the program limits were increased to enable a maximum feasible cut-off distance (R_{cut}) of 41 Å. Standard CHARMm allows a maximum R_{cut} of only 24 Å in case of the ephedrine–phosphoric acid salts.

(iii) To ensure convergence of the Coulomb term, the program was extended with an Ewald[57–59] summation. Analytical derivatives of the energy function in reciprocal space were not implemented, i.e., energy minimization with Ewald summation could not be performed.

(iv) All calculations were performed under periodic boundary conditions in which the neutral sphere requirement[60] was met by including complete (neutral) acid–base pairs only, i.e., if any atom of an acid–base pair lay within R_{cut} of the central unit cell, that whole acid–base pair was taken into account.

5.2 Results and discussion

Table 4 shows the contributions of the individual terms to the calculated lattice energies and the deviations between experimental and computed geometries for several values of the dielectric constant. Differences in lattice energy terms are summarized in Table 5. The MM calculated equivalent of ΔH_{solid} is denoted ΔE^{MM}_{solid}.

The geometries of the minimized diastereomeric salts are in good agreement with the X-ray results, in particular with a distance-dependent dielectric ($\epsilon = r_{ij}$, see Figure 4 for an example). This improvement over our previous calculations[20] must be attributed to the use of ESP charges. The ΔE^{MM}_{solid} values, however, deviate considerably from ΔH_{solid}. A significant difference in intramolecular energy (ΔE_{intra}) is computed for the diastereomeric pair with the unsubstituted acid when a distance-dependent dielectric ($\epsilon = r_{ij}$) is applied, which disagrees with the experimental results: the conformations of the ions are identical in both salts, and ΔE_{intra} should therefore be very small. This deviation does not occur in the other diastereomeric pair. Differences in VdW lattice energy contributions (ΔE_{VdW}) are in agreement with the results of the qualitative analyses (very small difference for the unsubstituted acid, and a significant difference for the 2-Cl substituted acid), except for $\epsilon = 4 \cdot r_{ij}$. A conclusion with respect to the actual value of ϵ is not possible on the basis of these results, as the geometric results suggest a distance-dependent dielectric function whereas the energetic results (ΔE_{intra} and ΔE_{VdW}) suggest a fixed dielectric constant ($\epsilon > 1$).

The Coulomb energy contribution has still not converged at a cut-off distance of 41 Å because of the large dipole moments of the asymmetric units (about 17 Debye with ESP derived charges) and the non-centrosymmetric space group ($P2_1$) of the structures. To ensure convergence of the electrostatic energy term, Ewald summation was employed. Results obtained for the 'best' force field optimized crystal structures (i.e., those obtained with $\epsilon = r_{ij}$ in Table 4) are shown in Table 6. The two rows labeled $\Delta E_{Coulomb}$ (comparing the results of the direct summation and the Ewald summation) show a different convergence behavior of the Coulomb energy in both pairs studied. Therefore, application of an Ewald summation is necessary to describe our diastereomeric salts more accurately, but it still does not improve the calculated energy differences to a sufficient level of reliability.

5.3 Perspectives and possible improvements

Analyses of the MM results showed that the mismatch between calculated and expected lattice energy differences is probably not caused by unreliable atomic charges or VdW parameters. The dielectric function ϵ, which is an already much debated source of problems in non solid state calculations, may be considered an even greater problem in this case. There might be a work-around by application of a more sophisticated function for ϵ, e.g., a sigmoidal distance-dependent dielectric,[61–64] but it should be realized that the dielectric constant in MM is at best a crude way to treat polarization, even with a

Table 4: Lattice Energy Minimizations. R_{cut} 41 Å; Gaussian-90 (6-31G** basis-set) ESP derived charges.

Salt [a]	Energy	Dielectric constant				
		5.0	8.0	12.0	r_{ij}	$4{\cdot}r_{ij}$
H n-salt	E^{MM}_{solid} [b]	-56.6	-43.7	-36.7	-114.3	-41.3
	E_{intra} [c]	12.0	11.9	11.8	14.5	11.4
	E_{VdW}	-33.6	-34.4	-34.7	-21.1	-31.5
	$E_{Coulomb}$	-35.0	-21.2	-13.8	-107.8	-21.2
H p-salt	E^{MM}_{solid}	-60.8	-46.9	-39.4	-121.6	-45.1
	E_{intra}	10.6	10.4	10.4	11.5	10.4
	E_{VdW}	-34.0	-34.5	-34.7	-21.1	-33.3
	$E_{Coulomb}$	-37.3	-22.9	-15.0	-112.1	-22.3
ΔE^{MM}_{solid}		4.2	3.2	2.7	7.3	3.8
Deviation from X-ray						
H n-salt	Δa (13.84 Å)[d]	-0.2	-0.4	-0.3	-0.3	-0.6
	Δb (7.80 Å)	-0.9	-1.2	-1.3	1.2	3.7
	Δc (10.17 Å)	0.6	0.9	1.1	-2.0	-1.8
	$\Delta\beta$ (93.0°)	-6.3	-8.0	-9.0	0.2	-1.7
	ΔVolume	-0.5	-0.8	-0.8	-1.2	1.4
	RMS fit (Å)[e]	0.44	0.52	0.57	0.36	0.40
H p-salt	Δa (14.00 Å)	0.9	0.7	0.5	1.7	1.0
	Δb (8.10 Å)	-4.1	-4.1	-4.0	-3.7	-3.7
	Δc (9.71 Å)	2.3	2.7	3.0	-0.3	1.4
	$\Delta\beta$ (98.9°)	-3.4	-3.4	-3.3	-0.9	-2.7
	ΔVolume	-0.4	-0.1	0.1	-2.2	-0.7
	RMS fit (Å)	0.36	0.37	0.38	0.33	0.38

---

[a] Substituent at the aromatic moiety of the acid (and salt type) are indicated.

[b] Energies are given in kcal/mol.

[c] E_{intra} is the sum of all "bonded" interactions, i.e., $E_{intra} = E_{bond} + E_{angle} + E_{torsion}$.

[d] Deviation of the calculated *a*, *b*, *c*, β and volume from the experimental values (%). Experimental unit cell parameters are given between parentheses.

[e] Mass weighted Root Mean Square fit between the X-ray coordinates and the CHARMm optimised structure, non-hydrogen atoms only.

Table 4: Lattice Energy Minimizations (continued).

Salt	Energy	Dielectric constant				
		5.0	8.0	12.0	r_{ij}	$4{\cdot}r_{ij}$
2-Cl n-salt	E^{MM}_{solid}	−57.9	−45.5	−38.7	−119.8	−45.5
	E_{intra}	12.0	12.0	12.0	13.1	12.0
	E_{VdW}	−36.5	−37.1	−37.3	−23.5	−36.0
	$E_{Coulomb}$	−33.5	−20.4	−13.4	−109.4	−21.5
2-Cl p-salt	E^{MM}_{solid}	−59.5	−45.6	−38.0	−120.3	−44.8
	E_{intra}	11.8	11.8	11.7	12.8	11.9
	E_{VdW}	−33.9	−34.4	−34.6	−21.0	−35.2
	$E_{Coulomb}$	−37.4	−22.9	−15.1	−112.1	−21.6
ΔE^{MM}_{solid}		1.6	0.1	−0.7	0.5	−0.7
Deviation from X-ray						
2-Cl n-salt	Δa (19.66 Å)	0.6	0.8	0.9	0.2	0.6
	Δb (7.21 Å)	1.5	1.5	1.5	−2.1	0.7
	Δc (7.92 Å)	−1.6	−1.5	−1.4	−1.4	−1.8
	$\Delta\beta$ (100.7°)	3.0	3.3	3.6	1.1	2.6
	ΔVolume	−0.8	−0.5	−0.4	−3.7	−1.5
	RMS fit (Å)	0.37	0.39	0.40	0.22	0.34
2-Cl p-salt	Δa (13.84 Å)	2.0	2.0	2.0	2.5	2.1
	Δb (8.38 Å)	−1.9	−2.0	−1.9	−1.3	0.4
	Δc (9.81 Å)	−0.8	−0.5	−0.4	−2.5	−4.8
	$\Delta\beta$ (99.7°)	−2.4	−2.6	−2.3	0.6	−0.1
	ΔVolume	−0.1	0.1	0.3	−1.7	−2.4
	RMS fit (Å)	0.40	0.41	0.41	0.38	0.55

Table 5: Differences in Lattice Energies.

Acid subst.	Energy [a] difference	Dielectric constant					ΔH_{solid} [b]
		5.0	8.0	12.0	r_{ij}	$4{\cdot}r_{ij}$	
H	ΔE^{MM}_{solid}	4.2	3.2	2.7	7.3	3.8	−0.1
	ΔE_{intra}	1.4	1.5	1.4	3.0	1.0	
	ΔE_{VdW}	0.4	0.1	0.0	0.0	1.8	
	$\Delta E_{Coulomb}$	2.3	1.7	1.2	4.3	1.1	
2-Cl	ΔE^{MM}_{solid}	1.6	0.1	−0.7	0.5	−0.7	−2.8
	ΔE_{intra}	0.2	0.2	0.3	0.3	0.1	
	ΔE_{VdW}	−2.6	−2.7	−2.7	−2.5	−0.8	
	$\Delta E_{Coulomb}$	3.9	2.5	1.7	2.7	0.1	

---

[a] The value of the p-salt was subtracted from the corresponding value of the n-salt.

[b] ΔH_{solid} is the expected value of ΔE^{MM}_{solid}.

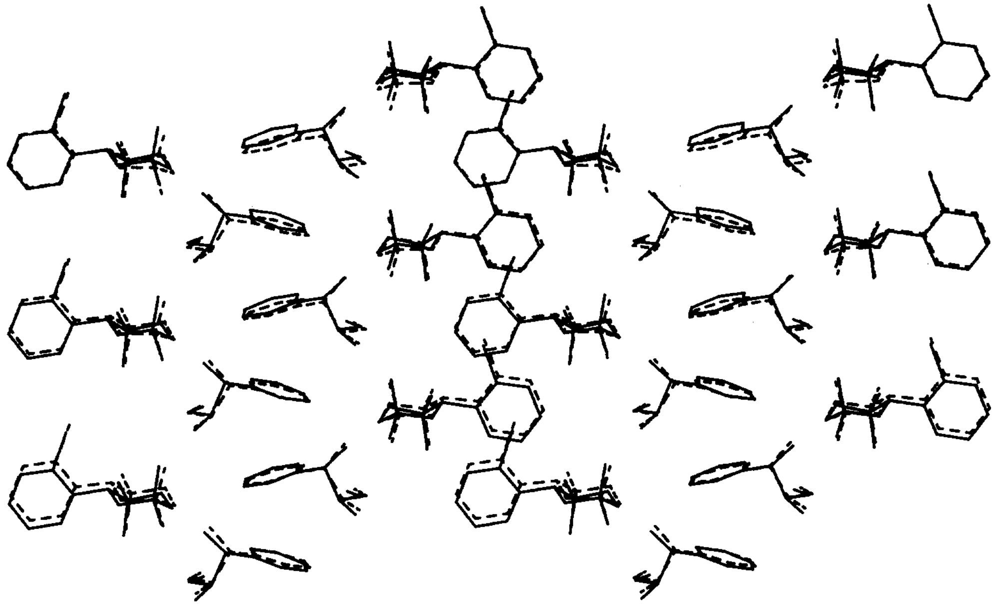

Figure 4: Superimposed experimental (solid lines) and force field minimized (dashed lines) crystal structures of the n-salt with the 2-Cl substituted phosphoric acid (ϵ = r_{ij}, RMS-fit = 0.22 Å). View perpendicular to the *ab* plane; hydrogen atoms were omitted.

'sophisticated' function for ϵ. These polarization effects play an important role in the ionic structures investigated here, and may well explain the unreliability of the MM results. For instance, it has been shown for ion–water clusters consisting of 1 to 6 water molecules and several monovalent ions (e.g., Li^+ and Cl^-) that between 10% and 25% of the total intermolecular energy is due to polarization.[65–68] It is easy to imagine that polarization effects differ for each type of crystal packing. In the diastereomeric pair with the 2-Cl substituted acid, for example, the difference in crystal packing is large (Class III versus Class I_p) and a considerable difference in polarization may occur. But even in the similarly packed pair with the 2-F substituted acid (Class I_n/Class I_p), subtle differences in interactions of the polarized aromatic systems probably lead to differences in polarization effects (see Section 4). From this point of view, the discrepancy between calculated and expected lattice energy differences may be understood.

Proper treatment of polarization may improve the reliability of the MM energy computations, and can be achieved by two extensions to the MM methodology. The first improvement involves the calculation of atomic charges. The Gaussian-ESP derived charges were computed for the separate — formally charged — ions *in vacuo*, but the salt-bridged ions are polarized in the crystal environment. 'Polarized' atomic charges may be obtained by performing an iterative series of Gaussian-ESP calculations on the ions surrounded by a set of point charges, which simulate the crystal environment. The second improvement consists of equipping the force field with properly parameterized polarization potentials. Such potentials are being developed,[69–73] but their parameterization is not trivial due to the non-additive

Table 4: Lattice Energy Minimizations (continued).

Salt	Energy	Dielectric constant				
		5.0	8.0	12.0	r_{ij}	$4 \cdot r_{ij}$
2-Cl n-salt	E^{MM}_{solid}	−57.9	−45.5	−38.7	−119.8	−45.5
	E_{intra}	12.0	12.0	12.0	13.1	12.0
	E_{VdW}	−36.5	−37.1	−37.3	−23.5	−36.0
	$E_{Coulomb}$	−33.5	−20.4	−13.4	−109.4	−21.5
2-Cl p-salt	E^{MM}_{solid}	−59.5	−45.6	−38.0	−120.3	−44.8
	E_{intra}	11.8	11.8	11.7	12.8	11.9
	E_{VdW}	−33.9	−34.4	−34.6	−21.0	−35.2
	$E_{Coulomb}$	−37.4	−22.9	−15.1	−112.1	−21.6
ΔE^{MM}_{solid}		1.6	0.1	−0.7	0.5	−0.7
Deviation from X-ray						
2-Cl n-salt	Δa (19.66 Å)	0.6	0.8	0.9	0.2	0.6
	Δb (7.21 Å)	1.5	1.5	1.5	−2.1	0.7
	Δc (7.92 Å)	−1.6	−1.5	−1.4	−1.4	−1.8
	$\Delta \beta$ (100.7°)	3.0	3.3	3.6	1.1	2.6
	ΔVolume	−0.8	−0.5	−0.4	−3.7	−1.5
	RMS fit (Å)	0.37	0.39	0.40	0.22	0.34
2-Cl p-salt	Δa (13.84 Å)	2.0	2.0	2.0	2.5	2.1
	Δb (8.38 Å)	−1.9	−2.0	−1.9	−1.3	0.4
	Δc (9.81 Å)	−0.8	−0.5	−0.4	−2.5	−4.8
	$\Delta \beta$ (99.7°)	−2.4	−2.6	−2.3	0.6	−0.1
	ΔVolume	−0.1	0.1	0.3	−1.7	−2.4
	RMS fit (Å)	0.40	0.41	0.41	0.38	0.55

Table 5: Differences in Lattice Energies.

Acid subst.	Energy [a] difference	Dielectric constant					ΔH_{solid} [b]
		5.0	8.0	12.0	r_{ij}	$4 \cdot r_{ij}$	
H	ΔE^{MM}_{solid}	4.2	3.2	2.7	7.3	3.8	−0.1
	ΔE_{intra}	1.4	1.5	1.4	3.0	1.0	
	ΔE_{VdW}	0.4	0.1	0.0	0.0	1.8	
	$\Delta E_{Coulomb}$	2.3	1.7	1.2	4.3	1.1	
2-Cl	ΔE^{MM}_{solid}	1.6	0.1	−0.7	0.5	−0.7	−2.8
	ΔE_{intra}	0.2	0.2	0.3	0.3	0.1	
	ΔE_{VdW}	−2.6	−2.7	−2.7	−2.5	−0.8	
	$\Delta E_{Coulomb}$	3.9	2.5	1.7	2.7	0.1	

---

[a] The value of the p-salt was subtracted from the corresponding value of the n-salt.

[b] ΔH_{solid} is the expected value of ΔE^{MM}_{solid}.

6 — TOWARDS A TRULY PREDICTIVE MODEL

Both the qualitative and the quantitative approaches rely on known X-ray structures. A truly predictive model describing racemate resolution via crystallization of diastereomeric salts should not rely on any experimental data, necessitating the use of a method to predict crystal packing (provided future developments will increase the reliability of MM). Computational methods dealing with crystal geometry optimization are well developed,[58,77,78] but they do not tackle the crystal packing problem itself since they invariably rely on the existence of a reasonable starting structure for the minimization procedure. However, the problem seems to be solved for simple hydrocarbons.[79–81] Recently, a new generally applicable packing method based on a modified Monte Carlo simulated annealing method has been proposed.[82] The first results of this approach to predict the crystal packing of some non-trivial hetero-atom containing organic molecules are rather impressive.[83–85]

Can this method be applied to predict the crystal structures of pairs of diastereomeric salts, and in conjunction with that, the resolution efficiency? In theory the answer is positive, but there are practical aspects which make the solution difficult and very elaborate. For instance, packing of diastereomers would involve bimolecular units, which have various internal degrees of freedom, in stead of single molecules with limited flexibility. In addition, to scout several potential resolving agents for a particular racemate would require the prediction of numerous crystal structures. Consequently, such a study would consume enormous computer resources, and probably costs more time and money than the traditional trial and error approach to establish a new resolution. In due course of time, however, it seems justified to assume that it will be possible and economically interesting to compute resolution efficiency "*ab initio*".

7 — CONCLUSIONS

(1) A resolution efficiency parameter $\ln(c_p/c_n)$, which is related to the difference in Gibbs free energy of solvation in a diastereomeric salt-pair ($\Delta\Delta G_{solv}$), is introduced.

(2) Thermodynamic considerations show that $\Delta\Delta G_{solv}$ can be approximated by the computationally accessible lattice enthalpy difference ΔH_{solid} in a diastereomeric salt-pair, allowing the calculation of the result of an optical resolution: $\Delta H_{solid} \approx -\ln(c_p/c_n)$.

(3) The above relationship was used qualitatively to rationalize six resolutions.

(4) Attempts to calculate ΔH_{solid} as a parameter for resolution efficiency show that present molecular mechanics techniques (including *ab initio* electrostatic potential derived atomic charges and Ewald summation in the Coulomb term) are not sufficiently reliable to compute accurate ΔH_{solid} values. Inclusion of properly parameterized polarization potentials may improve the computational results.

(5) Accurate experimental energy differences for a well-defined and unique series of complex organic solids are provided to improve and validate solid state force field calculations.

(6) Using future crystal packing calculations, a truly predictive model for racemate resolution via crystallization of diastereomeric salts has become possible.

8 — ACKNOWLEDGEMENTS

Thanks are due to Dr. A.D. van der Haest (Groningen Univ., Nijenborgh 4, NL-9747 AG Groningen) for the syntheses and the determination of the physico-chemical properties of the diastereomeric salts. We also thank Prof. A. Bruggink (DSM-Andeno BV, P.O. Box 81, NL-5900 AB Venlo), Dr. H.J. Bruins Slot (CAOS/CAMM Center, Toernooiveld, NL-6525 ED Nijmegen), Dr. G.J.A. Ariaans (Nijmegen Univ., Toernooiveld, NL-6525 ED Nijmegen) and Prof. H. Wynberg (Groningen Univ., Nijenborgh 4, NL-9747 AG Groningen) for valuable support. This investigation was supported (in part) by the Netherlands Foundation for Technical Research (STW) with financial aid from the Netherlands Foundation for the Advancement of Pure Research (NWO), project number GCH 66.0942. Use of the services and facilities of the Dutch CAOS/CAMM Center, under grant numbers SON 326-052 and STW NCH99.1751, is gratefully acknowledged.

9 — REFERENCES AND NOTES

1. Mason, S.F. *Chirality* **1989**, *1*, 183.
2. Enders, D.; Hoffmann, R.W. *Chemie in unserer Zeit* **1985**, *6*, 177.
3. Drayer, D.E. *Clin. Pharmacol. Ther.* **1986**, *40*, 125.
4. Ariëns, E.J.; Wuis, E.W.; Veringa, E.J. *Biochem. Pharmacol.* **1988**, *37*, 9.
5. Shindo, H.; Caldwell, J. *Chirality* **1991**, *3*, 91.
6. Crosby, J. *Tetrahedron* **1991**, *47*, 4789.
7. Blaser, H.-U. *Chem. Rev.* **1992**, *92*, 935.
8. Pasteur, L. *C.R. Hebd. Seances Acad. Sci.* **1853**, *37*, 162.
9. Lowry, T.M. *Optical Rotatory Power;* Dover Publications: New York. 1964.
10. Jacques, J.; Collet, A.; Wilen, S.H. *Enantiomers, Racemates and Resolutions;* Wiley-Interscience: New York. 1981.
11. Newman, P. *Optical Resolution Procedures for Chemical Compounds;* Vols. 1–3; Optical Resolution Information Center: New York. 1981.
12. Fogassy, E.; Faigl, F.; Ács, M.; Grofcsik, A. *J. Chem. Res. (S)* **1981**, p. 346.
13. Gould, R.O.; Gray, A.M.; Taylor, P.; Walkinshaw, M.D. *J. Am. Chem. Soc.* **198**, *107*, 5921.
14. Gorman, A.; Gould, R.O.; Gray, A.M.; Taylor, P.; Walkinshaw, M.D. *J. Chem. Soc. Perkin Trans. II* **1986**, p. 739.
15. Zingg, S.P.; Arnett, E.M.; McPhail, A.T.; Bothner-By, A.A.; Gilkerson, W.R. *J. Am. Chem. Soc.* **1988**, *110*, 1565.
16. Simon, K.; Kozsda, É.; Böcskei, Z.; Faigl, F.; Fogassy, E.; Reck, G. *J. Chem. Soc. Perkin Trans. II* **1990**, p. 1395.
17. ten Hoeve, W.; Wynberg, H. *J. Org. Chem.* **1985**, *50*, 4508.

18. van der Haest, A.D.; Wynberg, H.; Leusen, F.J.J.; Bruggink, A. *Recl. Trav. Chim. Pays-Bas* **1990**, *109*, 523.
19. Leusen, F.J.J.; Bruins Slot, H.J.; Noordik, J.H.; van der Haest, A.D.; Wynberg, H.; Bruggink, A. *Recl. Trav. Chim. Pays-Bas* **1991**, *110*, 13.
20. Leusen, F.J.J.; Bruins Slot, H.J.; Noordik, J.H.; van der Haest, A.D.; Wynberg, H.; Bruggink, A. *Recl. Trav. Chim. Pays-Bas* **1992**, *111*, 111.
21. van der Haest, A.D.; Wynberg, H.; Leusen, F.J.J.; Bruggink, A. *Recl. Trav. Chim. Pays-Bas* **1993**, *in press*.
22. α-[(1-methylamino)ethyl]benzyl alcohol; Ephedrine, isolated from *Ephedra sinica*, shows anti-allergenic activity and is structurally and physiologically related to adrenaline and noradrenaline[23]. The alkaloid is frequently used in resolutions[10,14,15].
23. Burger, A. In *The Basis of Medicinal Chemistry;* Part I; Wolff, M.E. Ed.; Wiley: New York, 1980; p. 1.
24. The two salts of a diastereomeric pair are denoted n-salt ((+−) or (−+) salt) and p-salt ((++) or (−−) salt)[25].
25. Ugi, I. *Z. für Natur Forschung* **1965**, *20b*, 405.
26. In *Handbook of Chemistry and Physics;* Weast, R.C. Ed.; CRC Press: Cleveland, 1974; p. D–126.
27. Kryuchkov, A.A.; Kozachenko, A.G.; Matrosov, E.I.; Kabachnik, M.I. *Izv. Akad. Nauk SSSR, Ser. Khim.* **1978**, p. 1985.
28. Cherkasov, R.A.; Ovchinnikov, V.V.; Pudovik, M.A.; Pudovik, A.N. *Usp. Khim.* **1982**, *51*, 1305.
29. Atkins, P.W. *Physical Chemistry;* Oxford University Press: Oxford. 1990.
30. Kozma, D.; Pokol, G.; Ács, M. *J. Chem. Soc. Perkin Trans. II* **1992**, p. 435.
31. Such free energy calculations (molecular dynamics) on ions in solid state and in solution would require immense computer resources. Furthermore, it is doubtful whether the results would be sufficiently accurate in view of the expected small energy differences $\Delta\Delta G_{solv}$.
32. Note that the sign of the free energy of solvation (from solid state to solution) is opposite to that of the lattice energy (defined as the energy gained by condensing a gas to a solid).
33. Our thermodynamic approach can be applied to other diastereomeric salt-pairs. The resulting (extensive) set of energetical data on non-trivial organic solids may prove a valuable tool in future force field development and validation.
34. Fogassy, E.; Ács, M.; Faigl, F.; Simon, K.; Rohonczy, J.; Ecsery, Z. *J. Chem. Soc. Perkin Trans. II* **1986**, p. 1881.
35. Gould, R.O.; Walkinshaw, M.D. *J. Am. Chem. Soc.* **1984**, *106*, 7840.
36. Brianso, M.C. *Acta Cryst.* **1981**, *B37*, 618.
37. Toda, F.; Mori, K.; Stein, Z.; Goldberg, I. *J. Org. Chem.* **1988**, *53*, 308.
38. Czugler, M.; Csöregh, I.; Kálmán, A.; Faigl, F.; Ács, M. *J. Mol. Struct.* **1989**, *196*, 157.
39. Kok, A.M.G.; Wynberg, H.; Smits, J.M.M.; Beurskens, P.T.; Parthasarathi, V. *Acta Cryst.* **1987**, *C43*, 1328.
40. Smits, J.M.M.; Beurskens, P.T.; Kok, A.M.G.; Wynberg, H. *Acta Cryst.* **1987**, *C43*, 1331.
41. Smits, J.M.M.; Beurskens, P.T.; Parthasarathi, V.; Rijk, E.A.V.; Kok, A.M.G.; Wynberg, H. *Acta Cryst.* **1987**, *C43*, 1334.

42. Kok, A.M.G.; Wynberg, H.; Parthasarathi, V.; Smits, J.M.M.; Beurskens, P.T. *Acta Cryst.* **1987**, *C43*, 1336.

43. Bruins Slot, H.J.; Leusen, F.J.J.; van der Haest, A.D.; van Bolhuis, F. *Acta Cryst.* **1992**, *C48*, 587.

44. Bruins Slot, H.J.; Leusen, F.J.J.; van der Haest, A.D.; Smits, J.M.M. *Acta Cryst.* **1992**, *C48*, 372.

45. Bruins Slot, H.J.; Leusen, F.J.J.; van der Haest, A.D.; van Bolhuis, F. *Acta Cryst.* **1992**, *C48*, 925.

46. The inter-layer distance is the shortest distance between the planes defined by the atoms of two adjacent hydrophobic layers. It is easily calculated from the unit cell parameters: distance = $\frac{d}{n} \cdot \sin\beta$, where d is the length of the crystallographic axis perpendicular to the layers, n is the number of hydrophobic layers per d Å, and β is the angle between unit cell vectors a and c.

47. Brooks, B.R.; Bruccoleri, R.E.; Olafson, B.D.; States, D.J.; Swaminathan, S.; Karplus, M. *J. Comput. Chem.* **1983**, *4*, 187.

48. Smith, J.C.; Karplus, M. *J. Am. Chem. Soc.* **1992**, *114*, 801.

49. This program is developed at the laboratories of Ciba-Geigy AG (Basel, Switzerland) to generate possible crystal structures of organic molecules. All computations were performed on an IBM RS-6000/550 workstation.

50. Singh, U.C.; Kollman, P.A. *J. Comput. Chem.* **1984**, *5*, 129.

51. Williams, D.E. In *Reviews in Computational Chemistry;* Vol. 2; Lipkowitz, K.B.; Boyd, D.B. Eds.; VCH Publishers: New York, 1991; p. 219.

52. Merz Jr., K.M. *J. Comput. Chem.* **1992**, *13*, 749.

53. Frisch, M.J.; Head-Gordon, M.; Trucks, G.W.; Foresman, J.B.; Schlegel, H.B.; Raghavachari, K.; Robb, M.A.; Binkley, J.S.; Gonzalez, C.; Defrees, D.J.; Fox, D.J.; Whiteside, R.A.; Seeger, R.; Melius, C.F.; Baker, J.; Martin, R.L.; Kahn, L.R.; Stewart, J.J.P.; Topiol, S.; Pople, J.A. GAUSSIAN is a product of Gaussian Inc., Pittsburgh PA (1990).

54. Williams, D.E.; QCPE program 568.

55. Williams, D.E. *J. Comput. Chem.* **1988**, *9*, 745.

56. Quanta/CHARMm Molecular Modeling Software, distributed by Molecular Simulations Inc., 16 New England Executive Park, Burlington, MA 01803-5297, U.S.A.

57. Ewald, P.P. *Ann. Physik* **1921**, *64*, 253.

58. Williams, D.E. *Topics in Current Physics* **1981**, *26*, 3.

59. Gdanitz, R.J.; In-house software of Ciba-Geigy AG.

60. Karfunkel, H.R. *J. Comput. Chem.* **1987**, *8*, 174.

61. Hingerty, B.E.; Ritchie, R.H.; Ferrell, T.L.; Turner, J.E. *Biopolymers* **1985**, *24*, 427.

62. Ramstein, J.; Lavery, R. *Proc. Natl. Acad. Sci. USA* **1988**, *85*, 7231.

63. Daggett, V.; Kollman, P.A.; Kuntz, I.D. *Biopolymers* **1991**, *31*, 285.

64. Mazur, J.; Jernigan, R.L. *Biopolymers* **1991**, *31*, 1615.

65. Cieplak, P.; Lybrand, T.P.; Kollman, P.A. *J. Chem. Phys.* **1987**, *86*, 6393.

66. Berne, B.J.; Wallqvist, A. *J. Chem. Phys.* **1988**, *88*, 8016.

67. Kollman, P.A.; Lybrand, T.P.; Cieplak, P. *J. Chem. Phys.* **1988**, *88*, 8017.

68. Caldwell, J.; Dang, L.X.; Kollman, P.A. *J. Am. Chem. Soc.* **1990**, *112*, 9144.

69. Caillet, J.; Claverie, P. *Acta Cryst.* **1975**, *A31*, 448.

70. Howard, A.E.; Singh, U.C.; Billeter, M.; Kollman, P.A. *J. Am. Chem. Soc.* **1988**, *110*, 6984.

71. van Gunsteren, W.F.; Berendsen, H.J.C. *Angew. Chem.* **1990**, *102*, 1020.

72. Dang, L.X.; Rice, J.E.; Caldwell, J.; Kollman, P.A. *J. Am. Chem. Soc.* **1991**, *113*, 2481.

73. Voisin, C.; Cartier, A.; Rivail, J.-L. *J. Phys. Chem.* **1992**, *96*, 7966.

74. Alemán, C.; Canela, E.I.; Franco, R.; Orozco, M. *J. Comput. Chem.* **1991**, *12*, 664.

75. Dillen, J.L.M. *J. Comput. Chem.* **1992**, *13*, 257.

76. Veenstra, D.L.; Ferguson, D.M.; Kollman, P.A. *J. Comput. Chem.* **1992**, *13*, 971.

77. Brünger, A.T.; Kuriyan, J.; Karplus, M. *Science* **1987**, *235*, 458.

78. Fujinaga, M.; Gros, P.; van Gunsteren, W.F. *J. Appl. Cryst.* **1989**, *22*, 1.

79. Perstin, A.J.; Kitaigorodsky, A.I. *The Atom-Atom Potential Method;* Springer Verlag: Heidelberg. 1987.

80. Gavezzotti, A. *J. Am. Chem. Soc.* **1989**, *111*, 1835.

81. Gavezzotti, A. *J. Am. Chem. Soc.* **1991**, *113*, 4622.

82. Gdanitz, R.J. *Chem. Phys. Lett.* **1992**, *190*, 391.

83. Karfunkel, H.R.; Gdanitz, R.J. *J. Comput. Chem.* **1992**, *13*, 1171.

84. Karfunkel, H.R.; Leusen, F.J.J. *Speedup* **1992**, *6*, 43.

85. Karfunkel, H.R.; Rohde, B.; Leusen, F.J.J.; Gdanitz, R.J.; Rihs, G. *J. Comput. Chem.* **1993**, *in press*.